J Stat Phys (2012) 149:10–36
DOI 10.1007/s10955-012-0573-z

Finite-Size Left-Passage Probability in Percolation

Yacine Ikhlef · Anita K. Ponsaing

Received: 1 June 2012 / Accepted: 17 August 2012 / Published online: 7 September 2012

Abstract We obtain an exact finite-size expression for the probability that a percolation hull will touch the boundary, on a strip of finite width. In terms of clusters, this corresponds to the one-arm probability. Our calculation is based on the q-deformed Knizhnik–Zamolodchikov approach, and the results are expressed in terms of symplectic characters. In the large size limit, we recover the scaling behaviour predicted by Schramm's left-passage formula. We also derive a general relation between the left-passage probability in the Fortuin–Kasteleyn cluster model and the magnetisation profile in the open XXZ chain with diagonal, complex boundary terms.

Keywords Percolation · SLE · Exact correlation functions · Temperley–Lieb algebra · XXZ model

1 Introduction

Percolation models in two dimensions play an important role both in theoretical physics and mathematics. On the physics side, it was one of the first models where the Coulomb gas approach [9, 20] was used to predict the critical exponents [24], and where the concepts of boundary conformal field theory (CFT) were put in practice [4]. Nowadays, it still attracts the community's attention, especially for its relation to logarithmic CFT. On the mathematics side, many rigorous studies of percolation have been pursued [29], and it has been proved [27] that site percolation on the triangular lattice has a conformally invariant scaling limit, described by Schramm–Loewner evolution (SLE) with $\kappa = 6$. Also, in combinatorics, the Razumov–Stroganov relation [3, 21, 22] identifies the components of the percolation transfer matrix eigenvector with the enumeration of plane partitions and alternating sign matrices.

Y. Ikhlef · A.K. Ponsaing (✉)
Section de Mathématiques, University of Geneva, Rue du Lièvre 2-4, Geneva, Switzerland
e-mail: Anita.Ponsaing@unige.ch

Y. Ikhlef
e-mail: Yacine.Ikhlef@unige.ch

The main objects of study in percolation are the percolation clusters and the lattice curves surrounding them, known as hulls. In the scaling limit, the correlation functions of these hulls are conjectured [24] to be described by a Coulomb gas CFT [9, 20], and thus to satisfy some partial differential equations (PDEs) given by the "null-vector equations". Some of these PDEs can be solved explicitly, e.g., the equation for the crossing probability (the probability that a cluster connects two sides of a rectangle) [4]. A very fruitful approach to relate CFT and SLE is to express the null-state equations of CFT as martingale conditions for the SLE observables [1, 5].

The left-passage probability $P_{\text{left}}(z)$, i.e., the probability for an open, oriented hull to pass to the left of a fixed point z of the system, is one of these observables that can be easily obtained for percolation (and more generally, for the Potts and O(n) models) both from the CFT and SLE viewpoints. In the SLE literature, this result is known as *Schramm's formula* [25]. In this paper, we address the determination of P_{left} *on the lattice*, in the infinite strip geometry, using rigorous techniques based on the Yang–Baxter and quantum Knizhnik–Zamolodchikov (qKZ) equations, as well as the Bethe ansatz for the related six-vertex model.

The qKZ approach is particularly powerful for loop models with a trivial partition function $\mathcal{Z} = 1$ [7, 12, 15, 16, 31]. In several cases, it allows the explicit determination of the dominant transfer matrix eigenvector, and it turns out that the components of this vector are integers enumerating plane partitions and alternating sign matrices. Also, the qKZ approach was recently used by one of the present authors to calculate a finite-size correlation function in percolation, namely the "transverse current" across a strip [13]. A complementary approach, with a larger scope, is to map a loop model onto an integrable spin chain [2], and use the Bethe ansatz to obtain correlation functions in the form of determinants [18, 19]. This approach extends to the Fortuin–Kasteleyn (FK) cluster model with cluster weight Q, and the percolation model is recovered for $Q = 1$.

The layout of this paper is as follows. In Sect. 2, we recall the exact equivalence [2] between bond percolation on the square lattice and the Temperley–Lieb loop model with weight $n = 1$, then briefly review its conjectured relation to SLE$_6$, and finally state our main results. In Sect. 3, we set up our notation for the transfer matrix and recall the basic steps of the qKZ approach. In Sect. 4 we derive explicitly, for a finite strip of odd width L, the probability $P_{\text{left}}(z)$ with z on the boundary of the strip. For a homogeneous system, we obtain fractional numbers with a simple combinatorial interpretation. In the large-L limit, we recover the power law predicted by CFT and SLE. In Sect. 5, we generalise to a generic point z: it turns out that similar symmetry and recursion relations hold, but are very difficult to solve in practice. However, we obtain two promising results in this case. First, we calculate $P_{\text{left}}(z)$ numerically for homogeneous systems with up to $L = 21$ sites, and observe good convergence to Schramm's formula. Second, we prove that, in the FK model, $P_{\text{left}}(z)$ relates very simply to the magnetisation profile in an open XXZ spin chain with diagonal, complex boundary terms. We give our conclusions and discuss open problems in Sect. 6.

2 Percolation, Temperley–Lieb Loops and SLE

2.1 Percolation Hulls and Their Scaling Exponents

Consider a square lattice $\mathcal{L}$, on which each edge can be occupied by a bond with probability p, or empty with probability $(1 - p)$. The connected components of the graph formed by all the sites and the occupied edges are called percolation clusters. We now look at the

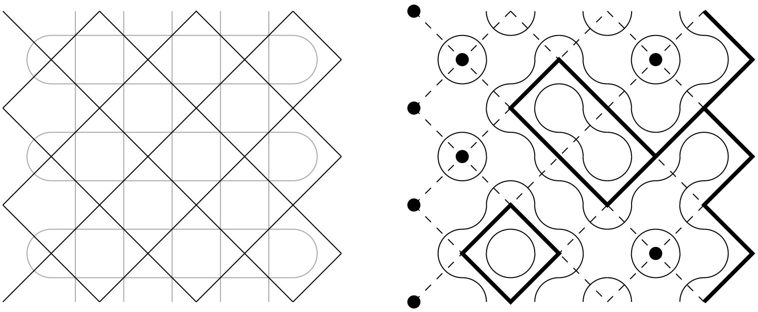

Fig. 1 *Left*: the original lattice $\mathcal{L}$ where bond percolation is defined (*black*) and its medial lattice $\mathcal{M}$ (*grey*). *Right*: an example cluster configuration (*thick lines* and *dots*) and the associated loop configuration (*thin lines*). On the *left* (resp. *right*) boundary, all edges are empty (resp. occupied)

medial lattice $\mathcal{M}$ formed by the mid-edges of $\mathcal{L}$, where a loop configuration is associated to each cluster configuration [2] (see Fig. 1). These loops follow the external boundaries and the internal cycles of the clusters, and are called the percolation hulls. The loop model describing these hulls is called the Temperley–Lieb loop model after its underlying algebra (see Sect. 3).

As usual, the scaling limit is defined by fixing a domain Ω of the plane, covering it with a square lattice of spacing a, then letting $a \to 0$. The scaling properties of percolation hulls at the critical point $p_c = 1/2$ can be determined by the Coulomb gas approach [20, 24], yielding the ℓ-leg "watermelon" exponents $X_\ell = (\ell^2 - 1)/12$, the fractal dimension $d_f = 7/4$, and the correlation-length exponent $\nu = 4/7$.

2.2 Strip Geometry and the SLE Model

We suppose that the system is defined on an infinite strip of $\mathcal{M}$, of width L, and we assume that L is odd. Let us specify the boundary conditions (BCs) that shall be used throughout the paper. On one boundary, we set all the edges of $\mathcal{L}$ to be occupied (wired BC), and on the other boundary, all edges are empty (free BC). This simply means the hulls must reflect on both boundaries. Since L is odd, there exists an infinite open hull propagating along the strip, which we shall denote γ (see Fig. 2). This open hull is the left boundary of the cluster attached to the right boundary of the strip.

In the scaling limit, the random curve γ is conjectured to be distributed as chordal $\mathrm{SLE}_{\kappa=6}$. For the SLE model, Schramm [25] obtained the left-passage probability P_{left} by solving an ordinary differential equation of order two. If we normalise the width of the strip to $L \times a = 1$ and denote by $x \in [0, 1]$ the horizontal coordinate, Schramm's formula reads

Theorem 2.1 (Schramm 2001, [25])

$$P_{\mathrm{left}}(x) = \frac{1}{2} - \frac{\Gamma(4/\kappa)}{\sqrt{\pi}\,\Gamma(\frac{8-\kappa}{2\kappa})} \operatorname{cotan}(\pi x)\ {}_2F_1\left(\frac{1}{2}; \frac{4}{\kappa}; \frac{3}{2}; -\operatorname{cotan}^2 \pi x\right), \tag{2.1}$$

where ${}_2F_1$ is the hypergeometric function.

This gives the probability of "touching" the boundary

$$P_{\mathrm{left}}(x) \underset{x\to 0}{\sim} \frac{\Gamma(4/\kappa)}{2\sqrt{\pi}\,\Gamma(\frac{8+\kappa}{2\kappa})} (\pi x)^{\frac{8-\kappa}{\kappa}}, \tag{2.2}$$

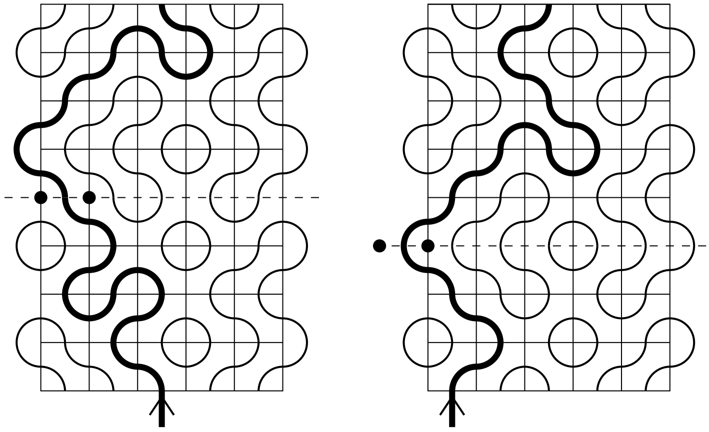

Fig. 2 (**a**) A configuration contributing to the boundary passage probability P_b on the selected section (*dotted line*). (**b**) A configuration contributing to the boundary passage probability $\widehat{P}_b$. In both cases, the *dots* indicate for which edge the passage probability is defined

with $\kappa = 6$ for percolation. Because of the above relation between γ and the cluster attached to the right boundary of the strip, the quantity (2.2) is exactly the one-arm probability in this geometry: this is the probability that a cluster connects the right boundary to a neighbourhood of the left boundary, of radius x.

In the present work, we derive some exact results for $P_{\text{left}}(x)$ in the lattice model, i.e., we look for analogs of (2.1) and (2.2) *in finite size*.

2.3 The Fortuin–Kasteleyn Cluster Model

Most of the above results can be generalised to $4 \le \kappa \le 8$ by considering a modified cluster model, called the Fortuin–Kasteleyn (FK) model, where each cluster gets a Boltzmann weight Q (the critical regime is $0 \le Q \le 4$), so that the Boltzmann weight of a cluster configuration C is

$$W[C] = Q^{\#\text{clusters(C)}} v^{\#\text{occupied edges(C)}}.$$

Loops are defined on the medial lattice similarly to percolation, and, using Euler's polyhedron formula for graphs, one finds that the above Boltzmann weight can be written as

$$W[C] \propto \sqrt{Q}^{\#\text{closed loops(C)}} \left(\frac{v}{\sqrt{Q}}\right)^{\#\text{occupied edges(C)}}.$$

This defines the Temperley–Lieb loop model with weight $n = \sqrt{Q}$ (see Sect. 3.1). It is conjectured (and proved for $Q = 2$) that the hulls of FK clusters are distributed in the scaling limit as SLE_κ with the relation

$$\sqrt{Q} = -2\cos\frac{4\pi}{\kappa}, \quad 4 \le \kappa \le 8.$$

2.4 Statement of Results

– In the percolation model with $n=-(q+q^{-1})$, using the qKZ approach, we obtain explicitly (see Sect. 4.4.1) the probability that the open path γ passes through a boundary edge.[1] There are two types of boundary edge, as the lattice rows come in pairs as can be seen in Fig. 3 (this pairing is reflected in the transfer matrix, see Definition 3.3). For a boundary edge in between two pairs of lattice rows, as depicted in Fig. 2a, the probability is

$$P_b(z_1,z_2,\dots,z_L)=\frac{\chi_{L-1}(z_2^2,\dots,z_L^2)\chi_{L+1}(z_1^2,z_1^2,z_2^2,\dots,z_L^2)}{\chi_L(z_1^2,\dots,z_L^2)^2},$$

and for a boundary edge in the middle of a pair of lattice rows, as depicted in Fig. 2b, it is

$$\begin{aligned}\widehat{P}_b(w;z_1,z_2,\dots,z_L)=&\frac{(q^{-1}-q)(w^2-w^{-2})}{\prod_{i=1}^L k(1/w,z_i)}\\&\times\frac{\chi_{L+1}(w^2,z_1^2,\dots,z_L^2)\chi_{L+1}((q/w)^2,z_1^2,\dots,z_L^2)}{\chi_L(z_1^2,\dots,z_L^2)^2}.\end{aligned}$$

In the above expressions, q has been set to $e^{2i\pi/3}$ (corresponding to $n=Q=1$), the z_j's are the vertical spectral parameters, w is the horizontal spectral parameter, χ_L is the symplectic character (see notations in Sect. 3), and we have defined

$$k(a,b):=(q/a)^2+(a/q)^2-b^2-b^{-2}.$$

– For a homogeneous percolation system (see Sect. 4.4.2), this becomes

$$P_b=\frac{A_V(L)A_V(L+2)}{N_8(L+1)^2},\quad\text{and}\quad\widehat{P}_b=\frac{3}{4^L}\frac{A(L)^2}{N_8(L+1)^2A_V(L)^2},$$

where $A(L)$, $A_V(L)$, and $N_8(L)$ are the number of $L\times L$ alternating sign matrices, $L\times L$ vertically symmetric alternating sign matrices, and $L\times L\times L$ cyclically symmetric self-complementary plane partitions respectively. Moreover, for a large system size L, both P_b and $\widehat{P}_b$ scale like $L^{-1/3}$ (see Sect. 4.4.3), which is consistent with (2.2) when $x=1/L$.

– In the critical Fortuin–Kasteleyn model with generic parameter $Q\in[0,4]$, we define the probability X_j that the path γ passes through the jth horizontal edge between two pairs of lattice rows. Figure 2a shows that $X_1=P_b$. We also define the left-passage probability P_{left} for any vertex between the two pairs of rows, and one can write

$$P_{\text{left}}(x_{j+1/2})-P_{\text{left}}(x_{j-1/2})=(-1)^{j-1}X_j,\quad\text{where } x_j:=j/L.$$

We find the relation (see Sect. 5.3)

$$X_j=(-1)^{j-1}\,\mathrm{Re}\left(\frac{\langle\Psi_0|\sigma_j^z|\Psi_0\rangle}{\langle\Psi_0|\Psi_0\rangle}\right),$$

[1] The term 'boundary edge' is used throughout this paper to mean the edge closest to the left boundary along the given row.

Fig. 3 The lattice with two reflecting boundaries

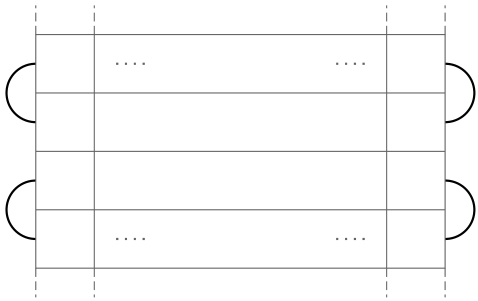

where $|\Psi_0\rangle$ is the groundstate eigenvector of the open XXZ Hamiltonian

$$\mathcal{H}_{\text{XXZ}} := \sum_{j=1}^{L-1}\left[\sigma_j^x\sigma_{j+1}^x + \sigma_j^y\sigma_{j+1}^y + \frac{1}{2}\left(q+q^{-1}\right)\sigma_j^z\sigma_{j+1}^z\right]$$
$$-\frac{1}{2}\left(q-q^{-1}\right)\left(\sigma_1^z - \sigma_L^z\right),$$

where q and Q are related by $\sqrt{Q} = -(q+q^{-1})$.

3 The qKZ Approach

3.1 The Temperley–Lieb Loop Model

The Temperley–Lieb loop model with wired (or reflecting) boundaries [7, 8, 11, 16] is defined on a square lattice, where each face is decorated with loops in one of the following two ways:

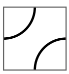 or .

Every closed loop gets a weight

$$n = -\left(q+q^{-1}\right).$$

We choose the boundary conditions for this model such that the lattice is infinite in height and of finite width L, and that the left and right boundaries are reflecting, as in Fig. 3.

Drawing a horizontal line across the width of the lattice, we consider the connectivities of the loops below the line while ignoring the paths the loops take, as well as any closed loops. We refer to this pattern of connectivities as a link pattern, and we denote by LP_L the set of link patterns for a given system width L. As explained in Sect. 2.2, we are only interested in odd system sizes $L = 2m-1$, for which the link patterns are enumerated by the mth Catalan number, $(2m)!/(m!(m+1)!)$. An example link pattern for $L = 7$ is

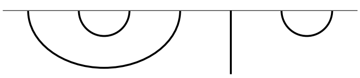.

We label the link patterns by $|\alpha\rangle$, using the shorthand notation of "$(\cdots)$" to indicate a pair of sites connected by a loop, and "|" to indicate the single unpaired loop that always exists in an odd-sized system. As an example, the above link pattern is indicated by $|\alpha\rangle = |(())|()\rangle$.

The link patterns for a fixed L form a representation of the Temperley–Lieb algebra, generated by $\{e_i, 1 \le i \le L-1\}$, with e_i depicted as

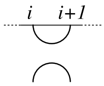

.

The relations for the Temperley–Lieb algebra are

$$\begin{aligned} e_i^2 &= n e_j, \\ e_i e_{i\pm 1} e_i &= e_i, \\ e_i e_j &= e_j e_i \quad \text{if } |i-j| > 1. \end{aligned} \tag{3.1}$$

Multiplication corresponds to concatenating the depictions of the generators, giving a weight of n to every closed loop, and disregarding the paths the loops take. In this way, we obtain relations between the link patterns such as $e_4|(())|()\rangle = ||()()()\rangle$ and $e_2|(())|()\rangle = n|(())|()\rangle$.

A state in $V_L = \mathrm{span}(\mathrm{LP}_L)$ is written as

$$|\phi\rangle = \sum_{\alpha \in \mathrm{LP}_L} \phi_\alpha |\alpha\rangle.$$

We look at all the possible configurations of two rows of the lattice, and consider how they send a given link pattern to another. We can write this as a matrix t that acts on V_L, and we refer to this as the transfer matrix.

We take an arbitrary initial state $|\mathrm{in}\rangle$ and act N times with the transfer matrix t. As $N \to \infty$, we get

$$\lim_{N\to\infty} t^N |\mathrm{in}\rangle \propto \Lambda^N |\Psi\rangle,$$

where Λ is the maximum eigenvalue of t and $|\Psi\rangle$ is the corresponding eigenvector, also known as the ground state. When $n = 1$ all the weights are probabilities and therefore $\Lambda = 1$. The components of $|\Psi\rangle$ can be thought of as the relative probabilities of the possible link patterns. In a similar way we define $\langle\Psi|$, which is the groundstate of the transfer matrix rotated by π, giving the relative probabilities of upward link patterns. The inner product between upward and downward link patterns is simply

$$\langle\beta|\alpha\rangle := n^{\#\text{closed loops}}, \quad \forall \alpha, \beta. \tag{3.2}$$

Hence, the expectation value of some observable $\mathcal{O}$ reads

$$\langle\mathcal{O}\rangle := \frac{\langle\Psi|\mathcal{O}|\Psi\rangle}{\langle\Psi|\Psi\rangle}.$$

3.2 The R-matrix

The possible states of each lattice square are described by the R-matrix. The definitions and properties here come from [7], with slightly different notation.

Definition 3.1

$$R(w,z) = $$ 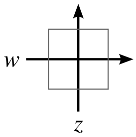

$$= \frac{[qz/w]}{[qw/z]}$$ 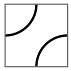 $$+ \frac{[z/w]}{[qw/z]}$$ 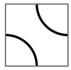 ,

where

$$[x] := x - 1/x.$$

Lemma 3.1 *This R-matrix satisfies the Yang–Baxter equation* (*YBE*), *depicted as*

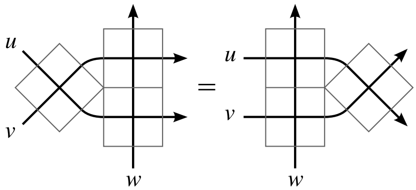

, (3.3)

the unitarity relation

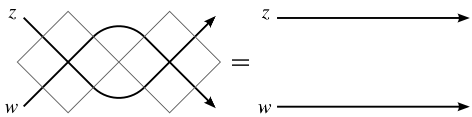

, (3.4)

and the crossing relation

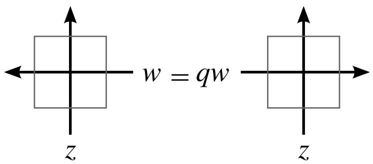

. (3.5)

Definition 3.2 The corresponding operator, acting from V_L to itself, is

$$\check{R}_j(w) := \frac{[q/w]}{[qw]}\mathbf{1} - \frac{[w]}{[qw]} e_j. \tag{3.6}$$

3.3 The Transfer Matrix, Symmetries and Recursions

We now define the transfer matrix t, which describes all the possible configurations of two lattice rows [7, 26]. Again all the relations given in this section come from [7].

Definition 3.3

$$t(w; z_1, \ldots, z_L) = \mathrm{Tr}_w\big[R(w,z_1)\ldots R(w,z_L)R(z_L,1/w)\ldots R(z_1,1/w)\big],$$

or pictorially,

$$t(w; z_1, \ldots, z_L) =$$ 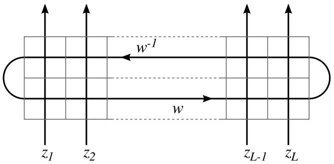

Lemma 3.2 *Thanks to the YBE* (3.3), *the transfer matrix satisfies the interlacing relation*

$$\check{R}_i(z_i/z_{i+1})t(w; z_i, z_{i+1}) = t(w; z_{i+1}, z_i)\check{R}_i(z_i/z_{i+1}), \tag{3.7}$$

pictorially,

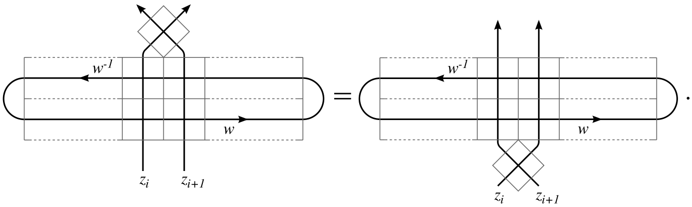

Considering the possible configurations of the two tiles at either position 1 *or position* L *of the transfer matrix also gives us*

$$\begin{aligned} t(w; z_1, z_2 \ldots) &= t(w; 1/z_1, z_2, \ldots), \\ t(w; \ldots, z_{L-1}, z_L) &= t(w; \ldots, z_{L-1}, 1/z_L), \end{aligned} \tag{3.8}$$

respectively.

Lemma 3.3 *By acting the transfer matrix on a small link from site* i *to* $i+1$ (*denoted by* φ_i) *and setting* $z_{i+1} = qz_i$ *we find the relation*

$$t_L(z_{i+1} = qz_i) \circ \varphi_i = \varphi_i \circ t_{L-2}(\hat{z}_i, \hat{z}_{i+1}), \tag{3.9}$$

where $\hat{z}$ *means that* z *is missing from the list of arguments.*

Proof Considering first the bottom row, we use the crossing relation (3.5) and then the unitarity relation (3.4):

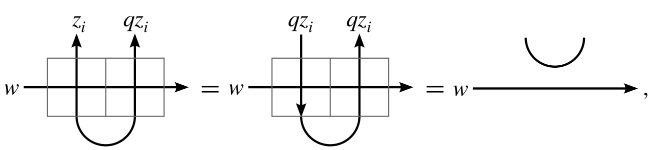

and see that the bottom row no longer depends on z_i and z_{i+1}. We repeat the procedure for the top row:

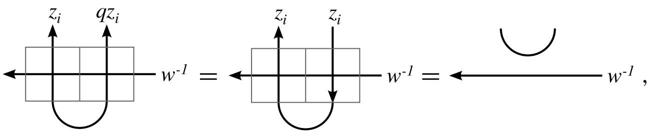

and the result follows. □

3.4 The Dominant Eigenvector

It is possible to show (see for example [7]) that two copies of the transfer matrix with different values of the parameter w commute, and therefore that the groundstate eigenvector does not depend on w. Explicitly, the eigenvalue equation is thus

$$t(w; z_1, \dots, z_L)\big|\Psi(z_1, \dots, z_L)\big\rangle = \big|\Psi(z_1, \dots, z_L)\big\rangle, \tag{3.10}$$

with the ground state eigenvector given by

$$\big|\Psi(z_1, \dots, z_L)\big\rangle = \sum_{\alpha\in \mathrm{LP}_L} \psi_\alpha(z_1, \dots, z_L)|\alpha\rangle.$$

From the expression for the R-matrix, the coefficients in the eigenvalue equation (3.10) are all rational functions of the z_j's, and hence one can normalise $|\Psi(z_1, \dots, z_L)\rangle$ so that all the components $\psi_\alpha(z_1, \dots, z_L)$ are Laurent polynomials in the z_j's. Moreover, one requires that these components have no common factor.

With this normalisation, the interlacing relations (3.7) and (3.8) yield the q-deformed Knizhnik–Zamolodchikov equation for the ground state eigenvector, expressed in the form

$$\begin{aligned} \check{R}_i(z_i/z_{i+1})\big|\Psi(z_1, \dots, z_L)\big\rangle &= \pi_i\big|\Psi(z_1, \dots, z_L)\big\rangle, \\ \big|\Psi(z_1, \dots, z_L)\big\rangle &= \big|\Psi(1/z_1, \dots, z_L)\big\rangle, \\ \big|\Psi(z_1, \dots, z_L)\big\rangle &= \big|\Psi(z_1, \dots, 1/z_L)\big\rangle, \end{aligned} \tag{3.11}$$

where $\pi_i f(z_i, z_{i+1}) = f(z_{i+1}, z_i)$.

Acting on $|\Psi_{L-2}(\hat{z}_i, \hat{z}_{i+1})\rangle$ with both sides of (3.9), we get

$$t_L(z_i, z_{i+1} = qz_i)\varphi_i\big|\Psi_{L-2}(\hat{z}_i, \hat{z}_{i+1})\big\rangle = \varphi_i\big|\Psi_{L-2}(\hat{z}_i, \hat{z}_{i+1})\big\rangle.$$

Since the ground state is unique, $|\Psi_L(z_{i+1} = qz_i)\rangle$ and $\varphi_i|\Psi_{L-2}(\hat{z}_i, \hat{z}_{i+1})\rangle$ are proportional, and one can show that $|\Psi\rangle$ satisfies the recursion relation

$$\big|\Psi_L(z_{i+1} = qz_i)\big\rangle = (-1)^L \prod_{j\notin\{i,i+1\}} k(z_i, z_j)\varphi_i\big|\Psi_{L-2}(\hat{z}_i, \hat{z}_{i+1})\big\rangle, \tag{3.12}$$

with

$$k(a, b) = [qb/a][q/ab].$$

3.5 Solution for the Eigenvector

The qKZ equation (3.11) forces certain symmetry requirements on the components of $|\Psi\rangle$, which lead to the solution for the ground state. For instance,

$$\psi_{|(\cdots()\cdots)} = (-1)^{\frac{L}{2}(\frac{L}{2}+1)} \prod_{1\le i<j\le \frac{L+1}{2}} k(z_j, z_i) \prod_{\frac{L+3}{2}\le i<j\le L} k(1/z_i, z_j).$$

By considering a path representation of the link patterns, one can write the other components in terms of factorised operators acting on this component. We will not give the explicit solution here as it is not needed for our calculations. A full explanation of the procedure is in Sect. 4.1 of [16].

3.6 The Normalisation Factor Z_L

The normalisation of the eigenvector is defined as

$$Z_L(z_1, \dots, z_L) := \sum_{\alpha\in \mathrm{LP}_L} \psi_\alpha(z_1, \dots, z_L).$$

The results in this section again come from [7]. To express Z_L, we first define the completely symmetric polynomial character of the symplectic group.

Definition 3.4 The symplectic character χ_λ associated to a partition $\lambda = (\lambda_1, \dots, \lambda_L)$ is given by

$$\chi_\lambda^{(L)}(u_1, \dots, u_L) = \frac{\det[u_i^{\mu_j} - u_i^{-\mu_j}]}{\det[u_i^{\delta_j} - u_i^{-\delta_j}]},$$

where $\delta_j = L - j + 1$ and $\mu_j = \lambda_j + \delta_j$.

Throughout this paper, we shall restrict to the partition $\lambda_j = \lfloor \frac{L-j}{2} \rfloor$, for which χ has the special recursion

$$\chi_\lambda^{(L)}\big(u_1^2, \dots, u_L^2\big)|_{u_i=qu_j} = (-1)^L \prod_{\ell\ne i,j} k(u_j, u_\ell)\chi_\lambda^{(L-2)}\big(\dots, \hat{u}_i^2, \dots, \hat{u}_j^2, \dots\big). \tag{3.13}$$

We will use the shorthand notation $\chi_L(\dots) := \chi_\lambda^{(L)}(\dots)$, with the particular choice of λ given above.

Proposition 3.4 *The normalisation Z_L is given by*

$$Z_L = \chi_L\big(z_1^2, \dots, z_L^2\big).$$

Proof The recursive property (3.12) of the ground state eigenvector is easily extended to its components, and thus to the normalisation,

$$Z_L(z_{i+1} = qz_i) = (-1)^L \prod_{\ell\ne i,i+1} k(z_i, z_\ell) Z_{L-2}(\hat{z}_i, \hat{z}_{i+1}). \tag{3.14}$$

As Z_L is a symmetric function (easily proven using (3.4) and the qKZ equation), this can be generalised to

$$Z_L(z_j = qz_i) = (-1)^L \prod_{\ell\neq i,j} k(z_i, z_\ell) Z_{L-2}(\hat{z}_i, \hat{z}_j).$$

The symplectic character $\chi_L(z_1^2, \dots, z_L^2)$ also satisfies these recursions, and it is straightforward to show that these recursions are enough to satisfy the degree of Z_L, which is set by solving the qKZ equation. It remains to show that the statement is true for $L = 1$ to initialise the recursion, which is done by observing that in this case both the left and the right hand side must be 1.[2] □

4 Boundary Passage Probabilities

When L is odd, all link patterns have an unpaired odd site. In the lattice this site belongs to an open path extending from $-\infty$ to ∞. In this section we will calculate two probabilities: P_b, the probability that this infinite path passes through the first site at a given vertical position (Fig. 2a); and $\widehat{P_b}$, the probability that this loop passes through the left boundary at a given vertical position (Fig. 2b).

4.1 Definitions

We first define $\langle\Psi|$ to be the ground state eigenvector of the transfer matrix rotated by π, given by

$$\langle\Psi| = \sum_{\alpha\in \mathrm{LP}_L} \bar{\psi}_{\bar{\alpha}} \langle\bar{\alpha}|,$$

and related to $|\Psi\rangle$ by

$$\bar{\psi}_{\bar{\alpha}}(z_1, \dots, z_L) = \psi_\alpha(z_L, \dots, z_1),$$

where $\bar{\alpha}$ is an upward link pattern, related to α by a rotation of π.

Definition 4.1 The first site passage probability is given by

$$P_b^{(L)} = \frac{\langle\Psi|\rho|\Psi\rangle}{\langle\Psi|\Psi\rangle}, \tag{4.1}$$

where ρ acts between a link pattern and a rotated link pattern,

$$\langle\beta|\rho|\alpha\rangle \in \{0, 1\},$$

giving 1 if the open path formed by these two link patterns goes through the first site, and 0 if it does not. For example, the following configuration has $\langle\beta|\rho|\alpha\rangle = 1$ (ρ is depicted as two dots marking the first site):

β

α

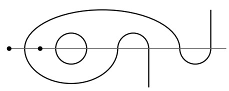

[2]Note that this proof is only valid for odd L; for even L the statement must also be proved for $L = 2$. We omit this part of the proof as we are only interested in odd system sizes.

Definition 4.2 The boundary passage probability $\widehat{P}^{(L)}$ is given by

$$\widehat{P}_b^{(L)} = \frac{\langle \Psi | \widehat{\rho} | \Psi \rangle}{\langle \Psi | \Psi \rangle}, \tag{4.2}$$

where $\widehat{\rho}$ marks out the left boundary loop in the transfer matrix. It is depicted as

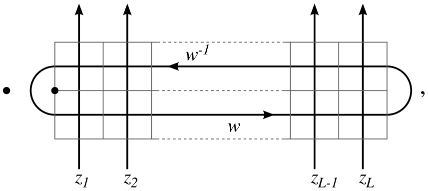

and like ρ, acts between an upward and a downward link pattern, multiplying each term in the transfer matrix by 1 if the infinite loop passes through the left boundary loop, and 0 if it does not. For example, the following configuration is multiplied by 1:

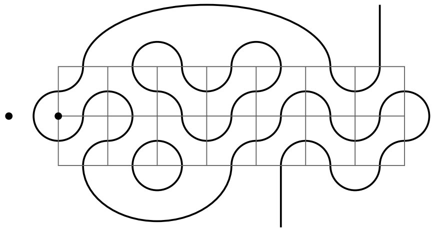

From (3.2) we have $\langle \beta | \alpha \rangle = 1, \forall \alpha, \beta$, so the denominators of $P_b^{(L)}$ and $\widehat{P}_b^{(L)}$ become

$$\langle \Psi | \Psi \rangle = \sum_{\alpha, \beta} \bar{\psi}_{\bar{\beta}} \psi_\alpha \langle \beta | \alpha \rangle = Z_L(z_L, \ldots, z_1) Z_L(z_1, \ldots, z_L) = \left[Z_L(z_1, \ldots, z_L) \right]^2.$$

Example ($L = 3$) For $L = 3$ there are two link patterns, $|()$ and $()|$. Solving the qKZ equation for the components of the eigenvector gives

$$\begin{aligned} \psi_{|()}(z_1, z_2, z_3) &= k(z_2, z_1), \\ \psi_{()|}(z_1, z_2, z_3) &= \frac{[q z_2/z_3]}{[z_2/z_3]} (1 - \pi_2) \psi_{|()}(z_1, z_2, z_3) \\ &= k(1/z_2, z_3), \end{aligned}$$

and $Z_3 = \psi_{|()} + \psi_{()|}$ is simply $\chi_3(z_1^2, z_2^2, z_3^2)$.

The only combination of upward and downward link patterns that does not contribute to $P_b^{(3)}$ is $\alpha = \bar{\beta} = ()|$. We thus find the first site passage probability by brute force as

$$\begin{aligned} P_b^{(3)} &= \frac{1}{Z_3^2} (\psi_{|()} \bar{\psi}_{|()} + \psi_{()|} \bar{\psi}_{|()} + \psi_{|()} \bar{\psi}_{()|}) \\ &= \frac{1}{Z_3^2} \big(\psi_{|()}(z_1, z_2, z_3) \psi_{()|}(z_3, z_2, z_1) + \psi_{()|}(z_1, z_2, z_3) \psi_{()|}(z_3, z_2, z_1) \end{aligned}$$

$$
\begin{aligned}
&+\psi_{|()}(z_1,z_2,z_3)\psi_{|()}(z_3,z_2,z_1)\big)\\
&=\frac{1}{Z_3^2}\big(5+z_1^4+z_1^{-4}+2\big(z_1^2z_2^2+z_1^2z_2^{-2}+z_1^{-2}z_2^2+z_1^{-2}z_2^{-2}+z_1^2z_3^2\\
&\quad+z_1^2z_3^{-2}+z_1^{-2}z_3^2+z_1^{-2}z_3^{-2}\big)+z_2^2z_3^2+z_2^2z_3^{-2}+z_2^{-2}z_3^2+z_2^{-2}z_3^{-2}\big).
\end{aligned}
$$

4.2 Symmetries

Proposition 4.1 *$P_b^{(L)}$ is symmetric in $z_2,\ldots,z_L$ and invariant under $z_i\to 1/z_i$ for $i\geq 2$.*

Proof This proof is similar to the proof that Z_L is symmetric, and uses the qKZ equation. Remembering that an $\check{R}$-matrix acting between sites $i\neq 1$ and $i+1$ commutes with ρ, we insert the identity $\check{R}_i(z_{i+1}/z_i)\check{R}_i(z_i/z_{i+1})$ into the definition for $P_b^{(L)}$:

$$
\begin{aligned}
P_b^{(L)}(\ldots z_i,z_{i+1}\ldots)&=\frac{\langle\Psi_L(z_i,z_{i+1})|\check{R}_i(z_{i+1}/z_i)\rho\check{R}_i(z_i/z_{i+1})|\Psi_L(z_i,z_{i+1})\rangle}{Z_L(z_i,z_{i+1})^2}\\
&=\frac{\langle\Psi_L(z_{i+1},z_i)|\rho|\Psi_L(z_{i+1},z_i)\rangle}{Z_L(z_{i+1},z_i)^2}\\
&=P_1^{(L)}(\ldots z_{i+1},z_i\ldots).
\end{aligned}
$$

The invariance of $P_b^{(L)}$ under $z_i\to 1/z_i$ simply follows from the invariance of $|\Psi_L\rangle$ and $\langle\Psi_L|$ under $z_L\to 1/z_L$, as well as the above symmetry. □

Proposition 4.2 *$\widehat{P}_b^{(L)}$ is symmetric in all the z_i's and invariant under $z_i\to 1/z_i$, $\forall i\in\{1,\ldots,L\}$.*

Proof The proof is similar to the previous proof, however it uses the fact that the interlacing condition (3.7) for the transfer matrix is also satisfied by $\widehat{\rho}$. □

4.3 Recursions

Proposition 4.3 *$P_b^{(L)}$ satisfies the following recursions*:

$$
\left.\begin{aligned}
P_b^{(L)}|_{z_L^2=(qz_k)^{\pm 2}}&=P_b^{(L-2)}(\hat{z}_k,\hat{z}_L),\\
P_b^{(L)}|_{z_L^2=(q/z_k)^{\pm 2}}&=P_b^{(L-2)}(\hat{z}_k,\hat{z}_L),
\end{aligned}\right\}\quad 1<k<L. \tag{4.3}
$$

Proof The denominator of $P_b^{(L)}$ has the recursion (3.14)

$$
Z_L\big(z_L^2=q^2z_{L-1}^2\big)^2=\prod_{i=1}^{L-2}k(z_{L-1},z_i)^2\,Z_{L-2}(z_1,\ldots,z_{L-2})^2,
$$

and we will show that the numerator has the same recursion factor.

From the recursion of the right eigenvector we have

$$\begin{aligned}\langle \Psi_L|\rho|\Psi_L\rangle|_{z_L^2=(qz_{L-1})^2} \\ &= \prod_{i=1}^{L-2} k(z_{L-1}, z_i)\big\langle \Psi_L\big(z_L^2 = q^2 z_{L-1}^2\big)\big|\rho\varphi_{L-1}\big|\Psi_{L-2}(z_1, \dots, z_{L-2})\big\rangle,\end{aligned}$$

and since ρ commutes with φ_{L-1}, we can consider $\langle \Psi_L|\varphi_{L-1}$, which is the π rotation of the vector $\varphi_1^\dagger|\Psi_L(z_L, \dots, z_1)\rangle$. Here, $\varphi_1^\dagger$ is the bottom half of the TL operator e_1, sending a link pattern of size L to one of size $L-2$. We can thus obtain our desired result by calculating $e_1|\Psi_L(z_L, \dots, z_1)\rangle$ and removing the resulting link from site 1 to site 2. Here the qKZ equation (3.11) comes in useful, as

$$\begin{aligned}\varphi_1\varphi_1^\dagger\big|\Psi_L(z_L, \dots, z_1)\big\rangle\big|_{z_L^2=(qz_{L-1})^2} \\ &= e_1\big|\Psi_L(z_L, \dots, z_1)\big\rangle\big|_{z_L^2=(qz_{L-1})^2} \\ &= -\left(\frac{[z_{L-1}/qz_L]}{[z_{L-1}/z_L]}\pi_{L-1} + \frac{[z_L/qz_{L-1}]}{[z_L/z_{L-1}]}\right)\big|\Psi_L(z_L, \dots, z_1)\big\rangle\Big|_{z_L^2=(qz_{L-1})^2} \\ &= -\frac{[q]}{[1/q]}\big|\Psi_L(z_{L-1}, qz_{L-1}, \dots, z_1)\big\rangle \\ &= \varphi_1\big|\Psi_{L-2}(z_{L-2}, \dots, z_1)\big\rangle\prod_{i=1}^{L-2} k(z_{L-1}, z_i).\end{aligned}$$

Therefore, we have

$$\varphi_1^\dagger\big|\Psi_L(z_L, \dots, z_1)\big\rangle\big|_{z_L^2=(qz_{L-1})^2} = \prod_{i=1}^{L-2} k(z_{L-1}, z_i)\big|\Psi_{L-2}(z_{L-2}, \dots, z_1)\big\rangle,$$

which is the π rotation of $\langle \Psi_{L-2}|\prod_{i=1}^{L-2} k(z_{L-1}, z_i)$, and thus,

$$\langle \Psi_L|\rho|\Psi_L\rangle|_{z_L^2=(qz_{L-1})^2} = \prod_{i=1}^{L-2} k(z_{L-1}, z_i)^2\langle \Psi_{L-2}|\rho_1|\Psi_{L-2}\rangle.$$

It follows that $P_b^{(L)}|_{z_L^2=(qz_{L-1})^2} = P_b^{(L-2)}$.

The other relations in (4.3) follow from the invariance of P_b under $z_i \leftrightarrow z_j$ and under $z_i \to 1/z_i$, for $i, j \neq 1$. □

Proposition 4.4 $\widehat{P}_b^{(L)}$ *satisfies the following recursions*:

$$\left.\begin{aligned}\widehat{P}_b^{(L)}|_{z_L^2=(qz_k)^{\pm 2}} &= \widehat{P}_b^{(L-2)}(\hat{z}_k, \hat{z}_L), \\ \widehat{P}_b^{(L)}|_{z_L^2=(q/z_k)^{\pm 2}} &= \widehat{P}_b^{(L-2)}(\hat{z}_k, \hat{z}_L),\end{aligned}\right\}\quad 1 \le k < L. \tag{4.4}$$

Proof This proof is similar to the previous one, but it also relies on the fact that $\widehat{\rho}$ satisfies the same recursion as the transfer matrix (3.9),

$$\widehat{\rho}^{(L)}(z_{i+1} = qz_i) \circ \varphi_i = \varphi_i \circ \widehat{\rho}^{(L-2)}(\hat{z}_i, \hat{z}_{i+1}).$$ □

4.4 Exact Solution

4.4.1 Inhomogeneous System

Proposition 4.5 *The explicit formula for the first site passage probability is*

$$P_b^{(L)} = \frac{\chi_{L-1}(z_2^2,\dots,z_L^2)\chi_{L+1}(z_1^2,z_1^2,z_2^2,\dots,z_L^2)}{\chi_L(z_1^2,\dots,z_L^2)^2}. \tag{4.5}$$

Proof There are three steps to this proof. First, the degree of the proposed expression is shown to agree with the definition. Second, enough recursions (or values of the polynomial at specified points) are found to satisfy the degree. Third, the proposed expression is shown to be true for a small size example ($L = 3$), to initialise the recursion.

The denominator of (4.1) can be easily shown to be Z_L^2, which has a degree of $L-1$ in each variable z_i^2, because L is always odd. The action of ρ can not raise the polynomial degree, so the numerator of $P_b^{(L)}$ must have, at most, the same degree as the denominator. The degree of the numerator of (4.5) is $(L-3)/2 + (L-1)/2 = L-2$ in each z_i^2, so this requirement is satisfied.[3]

We view $P_b^{(L)}$ as a polynomial in z_L^2 with coefficients in the other z_i's, and to satisfy the degree we must establish the value of the polynomial for at least $2L-1$ values of z_L^2 (remembering that it is a Laurent polynomial). The following recursions (from Proposition 4.3) will give the value of $P_B^{(L)}$ at $4(L-2)$ values of z_L^2, which is enough if $L \geq 5$:

$$\left.\begin{aligned} P_b^{(L)}|_{z_L^2=(qz_k)^{\pm 2}} &= P_b^{(L-2)}(\hat{z}_k,\hat{z}_L),\\ P_b^{(L)}|_{z_L^2=(q/z_k)^{\pm 2}} &= P_b^{(L-2)}(\hat{z}_k,\hat{z}_L),\end{aligned}\right\}\quad 1<k<L.$$

The proof that these recursions are satisfied by the proposed expression for $P_b^{(L)}$ is straightforward, based on the known recursions for χ (3.13).

It thus remains to show that the expression is true for $L = 3$,

$$P_b^{(3)} = \frac{\chi_4(z_1^2,z_1^2,z_2^2,z_3^2)}{\chi_3(z_1^2,z_2^2,z_3^2)^2},$$

which is done by brute force, as in Sect. 4.3. □

Proposition 4.6 *The explicit formula for the boundary passage probability is*

$$\widehat{P}_b^{(L)} = \frac{-[q][w^2]}{\prod_{i=1}^L k(1/w,z_i)}\ \frac{\chi_{L+1}(w^2,z_1^2,\dots,z_L^2)\chi_{L+1}((q/w)^2,z_1^2,\dots,z_L^2)}{\chi_L(z_1^2,\dots,z_L^2)^2}. \tag{4.6}$$

Proof This is a similar proof to the previous one, with the same three steps.

The denominator of (4.2) is Z_L^2 multiplied by the denominator of $\widehat{\rho}$, which is the same as the denominator of the transfer matrix; that is, $\prod_{i=1}^L k(1/w,z_i)$. Thus the degree of the

[3]The definition of the transfer matrix implies that the components of the eigenvector, and thus the passage probabilities, are only functions of z_i^2 and do not depend on any odd powers of z_i. This fact is crucial to these proofs.

denominator is L in each z_i^2. Again because of the definition of $\widehat{\rho}$ the numerator of $\widehat{P}_b^{(L)}$ will be at most the same as the denominator. The degree of the numerator of (4.6) is $2(L-1)/2 = L-1$ in each z_i^2.

We view $\widehat{P}_b^{(L)}$ as a polynomial in z_L^2 with coefficients in the other z_i's and w, and to satisfy the degree we need to know the value of the polynomial for at least $2L+1$ values of z_L^2. As in the previous proof, we list here recursions that will give the value of $\widehat{P}_b^{(L)}$ at $4(L-1)$ values of z_L^2, which is enough if $L \geq 3$. These recursions come from Proposition 4.4.

$$\left.\begin{aligned} \widehat{P}_b^{(L)}|_{z_L^2=(qz_k)^{\pm 2}} &= \widehat{P}_b^{(L-2)}(\hat{z}_k, \hat{z}_L), \\ \widehat{P}_b^{(L)}|_{z_L^2=(q/z_k)^{\pm 2}} &= \widehat{P}_b^{(L-2)}(\hat{z}_k, \hat{z}_L), \end{aligned}\right\} \quad 1 \leq k < L.$$

The proof that these recursions are satisfied by the proposed expression for $\widehat{P}_b^{(L)}$ is again based on the known recursions for χ (3.13), but also relies on properties of $k(a,b)$ that imply

$$\frac{k(z_k, w)k(z_k, q/w)}{k(1/w, z_k)k(1/w, qz_k)} = \frac{k(z_k/q, w)k(z_k/q, w/q)}{k(1/w, z_k)k(1/w, z_k, q)} = 1.$$

It thus remains to show that the expression is true for $L = 1$,

$$\widehat{P}_b^{(1)} \stackrel{?}{=} \frac{-[q][w^2]}{k(1/w, z_1)} \frac{\chi_2(w^2, z_1^2)\chi_2((q/w)^2, z_1^2)}{\chi_1(z_1^2)^2} = \frac{-[q][w^2]}{k(1/w, z_1)}.$$

There are four configurations of $\widehat{\rho}$, three of which contribute to $\widehat{P}_b^{(1)}$. The one that does not has a weight $([qz_1/w][q/z_1w])([qw/z_1][qz_1w])^{-1}$, so

$$\widehat{P}_b^{(1)} = 1 - \frac{[qz_1/w][q/z_1w]}{[qw/z_1][qz_1w]} = \frac{[qw/z_1][qz_1w] - [qz_1/w][q/z_1w]}{k(1/w, z_1)} = \frac{-[q][w^2]}{k(1/w, z_1)}. \qquad \square$$

4.4.2 Homogeneous Limit

In this section we use the homogeneous limit $z_1 = \cdots = z_L = 1$, $w^2 = -q$, which implies that the two orientations of the lattice faces each have a probability of $1/2$.

Proposition 4.7 *The expression for $P_b^{(L)}$ in the homogeneous limit is*

$$P_b^{(L)} = \frac{A_V(L)A_V(L+2)}{N_8(L+1)^2}, \tag{4.7}$$

where $A_V(L)$ is the number of $L \times L$ vertically symmetric alternating sign matrices and $N_8(L)$ is the number of cyclically symmetric self-complementary plane partitions of size $L \times L \times L$, and these have the explicit expressions

$$A_V(2m+1) = \prod_{i=0}^{m-1} \frac{(3i+2)(6i+3)!(2i+1)!}{(4i+2)!(4i+3)!},$$

$$N_8(2m) = \prod_{i=0}^{m-1} \frac{(3i+1)(6i)!(2i)!}{(4i)!(4i+1)!}.$$

Proof The result (4.7) is simply obtained from (4.5) and the homogeneous limit of the symplectic characters [8],

$$\chi_{2m}(1,\dots,1) = 3^{m(m-1)} A_V(2m+1),$$
$$\chi_{2m-1}(1,\dots,1) = 3^{(m-1)^2} N_8(2m). \qquad \square$$

Proposition 4.8 *The expression for $\widehat{P}_b^{(L)}$ in the homogeneous limit is*

$$\widehat{P}_b^{(L)} = \frac{3}{4^L} \frac{A(L)^2}{N_8(L+1)^2 A_V(L)^2}, \tag{4.8}$$

where $A(L)$ is the number of $L \times L$ alternating sign matrices,

$$A(L) = \prod_{i=0}^{L-1} \frac{(3i+1)!}{(L+i)!}.$$

Proof For $\widehat{P}_b^{(L)}$ in (4.6), taking the homogeneous limit gives us

$$\widehat{P}_b^{(L)} = \frac{(-3)}{(-4)^L} \frac{\chi_{L+1}(-q,1,\dots,1)^2}{3^{2(m-1)^2} N_8(L+1)^2},$$

where we have set $L = 2m-1$. To simplify the numerator, we use the relation [30]

$$s_\lambda^{(4m-2)}\big(u_1, u_1^{-1}, \dots, u_{2m-1}, u_{2m-1}^{-1}\big)$$
$$= \chi_{2m}(q, u_1, \dots, u_{2m-1}) \chi_{2m}(-q, u_1, \dots, u_{2m-1}),$$

where s_λ is the Schur function for the partition λ. The homogeneous expression for s_λ is [10]

$$s_\lambda^{(2L)}(1,\dots,1) = 3^{L(L-1)/2} A(L),$$

and thus $\chi_{L+1}(-q,1,\dots,1)$ becomes

$$\chi_{L+1}(-q,1,\dots,1) = \frac{3^{(2m-1)(m-1)} A(L)}{\chi_{L+1}(q,1,\dots,1)}.$$

We then use the recursion for $\chi_{L+1}(q,1,\dots,1)$ to get

$$\chi_{L+1}(-q,1,\dots,1) = \frac{3^{(2m-1)(m-1)} A(L)}{k(1,1)^{2m-2} \chi_{2m-2}(1,\dots,1)} = \frac{3^{(m-1)^2} A(L)}{A_V(L)},$$

from which the result (4.8) follows immediately. $\square$

4.4.3 Large-L Limit

Proposition 4.9 *In the limit $L \to \infty$, $P_b^{(L)}$ and $\widehat{P}_b^{(L)}$ as given in* (4.7) *and* (4.8) *have the asymptotic behaviour*

$$P_b^{(L)} \sim C L^{-1/3}, \qquad \widehat{P}_b^{(L)} \sim \widehat{C} L^{-1/3}, \tag{4.9}$$

where

$$C = \frac{92^{-5/3}\Gamma(1/3)\Gamma(5/6)}{\Gamma(1/6)\Gamma(2/3)}, \qquad \widehat{C} = \frac{2^{14/9}\pi^{1/3}G(1/3)^4G(5/6)^4}{G(1/2)^4G(2/3)^2}.$$

Hence, with the relationship $x = 1/L$, the lattice probabilities P_b and $\widehat{P}_b$ follow the limiting behaviour predicted by Schramm's formula (2.2) at $\kappa = 6$ with the correct exponent, but with different multiplicative constants. This is because P_b and $\widehat{P}_b$ correspond to fixing a position j and letting L tend to infinity, whereas the scaling limit would require a fixed ratio $x = \pi j/L$.

5 Left-Passage Probabilities

In the previous sections we calculated an exact expression for the passage probability through an edge on or next to the boundary of the lattice. In this section, we address the determination of P_{left} for a general position j. While we are not able to obtain an analytic expression for general L, we calculate numerics for systems up to $L = 21$ and analyse the convergence to Schramm's formula. In the latter part of the section we consider a mapping to an open XXZ spin chain.

5.1 Definitions and Properties

Definition 5.1 For $j \in \{1, \dots, L\}$, we denote by $X_j(z_1, \dots, z_L)$ the probability that the path γ passes through the j-th horizontal edge in a horizontal section of the type shown in Fig. 2a.

Definition 5.2 For $j \in \{0, \dots, L+1\}$, we denote by $\widehat{X}_j(w; z_1, \dots, z_L)$ the probability that the path γ passes through the j-th horizontal edge in a horizontal section of the type shown in Fig. 2b.

Definition 5.3 For $j \in \{1, \dots, L+1\}$, we denote by $Y_j(w; z_1, \dots, z_L)$ the probability that the path γ passes through the j-th vertical edge above a horizontal section of the type shown in Fig. 2a.[4]

Lemma 5.1 *Using the convention that the vertices on a horizontal section like in Fig. 2a are numbered* $\{1/2, \dots, L+1/2\}$, *the probability that* γ *passes to the left of* $(j+1/2)$ *is*

$$P_{j+1/2} = \sum_{\ell=1}^{j} (-1)^{\ell-1} X_\ell.$$

On a horizontal section like in Fig. 2b, the probability that γ *passes to the left of* $(j+1/2)$ *is*

$$\widehat{P}_{j+1/2} = \sum_{\ell=0}^{j} (-1)^{\ell} \widehat{X}_\ell.$$

In particular, we have $X_1 = P_{3/2} = P_b$ *and* $\widehat{X}_0 = \widehat{P}_{1/2} = Y_1 = \widehat{P}_b$.

[4] We could also define $\widehat{Y}_j$ in a similar fashion, but this is simply related to Y_j by the transformation $z_k \to 1/z_k$, $\forall k$.

The power of (-1) in the above sums can be explained in the following way. The infinite loop, oriented as in Fig. 2, can only pass in one direction through any given edge: For X_j, it passes upwards if j is odd and downwards if j is even; for $\widehat{X}_j$ the opposite is true. When calculating the left-passage probabilities all configurations with the path passing downwards through the edge must be counted with a negative sign.

Lemma 5.2 *The probabilities X, $\widehat{X}$ and Y are related by the conservation property*

$$\forall j \in \{1, \dots, L\}, \quad X_j + \widehat{X}_j = Y_j + Y_{j+1},$$

and the identities for special values of w

$$\begin{aligned} Y_j|_{w=z_j} &= \widehat{X}_j|_{w=z_j}, & Y_{j+1}|_{w=z_j} &= X_j, \\ Y_j|_{w=qz_j} &= X_j, & Y_{j+1}|_{w=qz_j} &= \widehat{X}_j|_{w=qz_j}. \end{aligned}$$

Proof The conservation property comes from considering the possible configurations on a face. Each X and Y has two terms corresponding to the two possible configurations, and for each X one of these terms matches one of those for one of the Ys. At the special values $w = z_j$ and $w = qz_j$, the face at position j is specialised to one of the configurations, and the identities follow immediately. □

Similarly to P_b and $\widehat{P}_b$, the probabilities X, $\widehat{X}$ and Y satisfy some symmetry and recursion relations.

Proposition 5.3 *The probabilities $X_j(z_1, \dots, z_L)$ and $\widehat{X}_j(w; z_1, \dots, z_L)$ are symmetric functions of $\{z_1, \dots, z_{j-1}\}$ and $\{z_{j+1}, \dots, z_L\}$ separately.*

$X_j(z_1, \dots, z_L)$ is invariant under $z_\ell \to 1/z_\ell$ for all ℓ, and $\widehat{X}_j(w; z_1, \dots, z_L)$ is invariant under $z_\ell \to 1/z_\ell$ for $\ell \neq j$.

The probability $Y_j(w; z_1, \dots, z_L)$ is a symmetric function of $\{z_1, \dots, z_{j-1}\}$ and $\{z_j, \dots, z_L\}$ separately, and invariant under $z_\ell \to 1/z_\ell$ for all ℓ.

Proof The proof is similar to those of Proposition 4.1 and Proposition 4.2. □

Proposition 5.4 *The probabilities $X_j(z_1, \dots, z_L)$ and $\widehat{X}_j(w; z_1, \dots, z_L)$ satisfy the recursion relations*

$$\left.\begin{aligned} X_j^{(L)}|_{z_1^2=(qz_\ell)^{\pm 2}} &= X_{j-2}^{(L-2)}(\hat{z}_1, \hat{z}_\ell), \\ \widehat{X}_j^{(L)}|_{z_1^2=(qz_\ell)^{\pm 2}} &= \widehat{X}_{j-2}^{(L-2)}(\hat{z}_1, \hat{z}_\ell), \end{aligned}\right\} \quad 1 < \ell < j,$$

$$\left.\begin{aligned} X_j^{(L)}|_{z_L^2=(qz_\ell)^{\pm 2}} &= X_j^{(L-2)}(\hat{z}_\ell, \hat{z}_L), \\ \widehat{X}_j^{(L)}|_{z_L^2=(qz_\ell)^{\pm 2}} &= \widehat{X}_j^{(L-2)}(\hat{z}_\ell, \hat{z}_L), \end{aligned}\right\} \quad j < \ell < L,$$

whereas $Y_j(w; z_1, \dots, z_L)$ satisfies

$$Y_j^{(L)}|_{z_1^2=(qz_\ell)^{\pm 2}} = Y_{j-2}^{(L-2)}(\hat{z}_1, \hat{z}_\ell), \quad \textit{for } 1 < \ell < j,$$

$$Y_j^{(L)}|_{z_L^2=(qz_\ell)^{\pm 2}} = Y_j^{(L-2)}(\hat{z}_\ell, \hat{z}_L), \quad \textit{for } j \le \ell < L.$$

Table 1 Left-passage probabilities $P_j^{(L)}$ for strips of width $L \leq 11$. Data obtained by numerical diagonalisation of the transfer matrix

L	Z_L	$P_j^{(L)} \times Z_L^2$
3	2	0, 3, 1, 4
5	11	0, 78, 22, 99, 43, 121
7	170	0, 16796, 4484, 21093, 7807, 24416, 12104, 28900
9	7429	0, 29641710, 7721790, 37074705, 12859293 ...
11	920460	0, 426943865250, 109785565350, 532943651700, 178807268772, 605036201854 ...

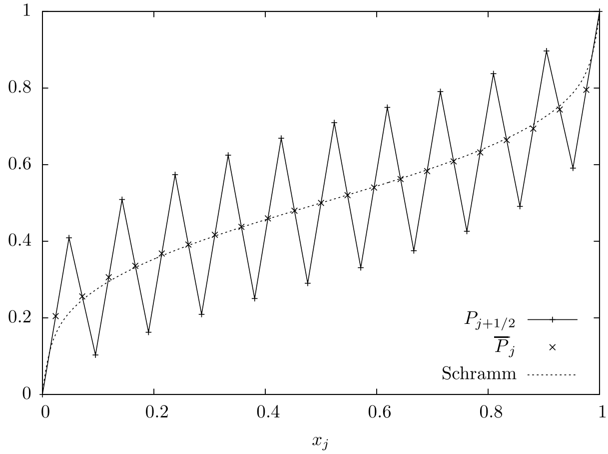

Fig. 4 The left-passage probability $P_{j+1/2}$ and its smooth part $\overline{P}_j$ for $L = 21$, compared to Schramm's formula (2.1)

Proof The proof is similar to those of Proposition 4.3 and Proposition 4.4. □

The above relations satisfied by X_j, $\widehat{X}_j$ and Y_j are, in principle, sufficient to determine completely these quantities. However, they turn out to be particularly difficult to solve in practice, and we resort to different tools to describe them.

5.2 Numerical Study

For a given choice of the z_j's, one can numerically find the components ψ_α by the power method, and use these to evaluate X_j, $\widehat{X}_j$ and Y_j directly. The left-passage probabilities are then obtained from Lemma 5.1. For small enough system sizes, we find the left-passage probabilities $P_{j+1/2}$ as fractions of integers (see Table 1).

We now turn to the convergence of $P_{j+1/2}$ to Schramm's formula (2.1). From Lemma 5.1, we see that $P_{j+1/2}$ is the sum of an alternating sequence, and has oscillations of wavelength $\delta j = 1$. This phenomenon appears clearly in Fig. 4. For this reason, we define the smooth and oscillatory parts as

$$\overline{P}_j := \frac{1}{2}(P_{j-1/2} + P_{j+1/2}), \qquad \widetilde{P}_j := \frac{1}{2}(P_{j-1/2} - P_{j+1/2}) = \frac{1}{2}(-1)^{j-1} X_j.$$

In Fig. 4 we see that $\overline{P}_j$ is very close to Schramm's formula for $L = 21$. In Fig. 5, we compare the data for $\overline{P}_j$ at various system sizes, and observe very good convergence to

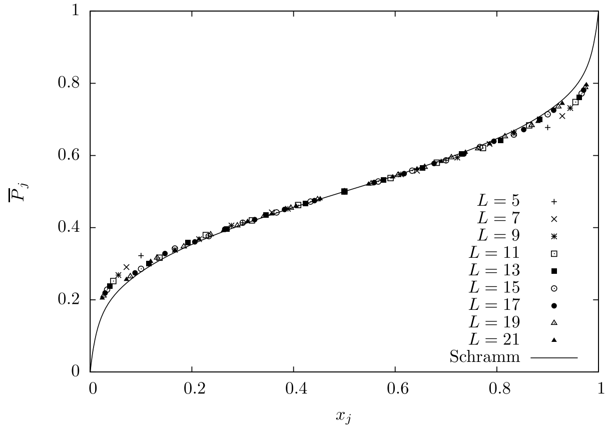

Fig. 5 Smooth part of the left-passage probability, compared to Schramm's formula (2.1)

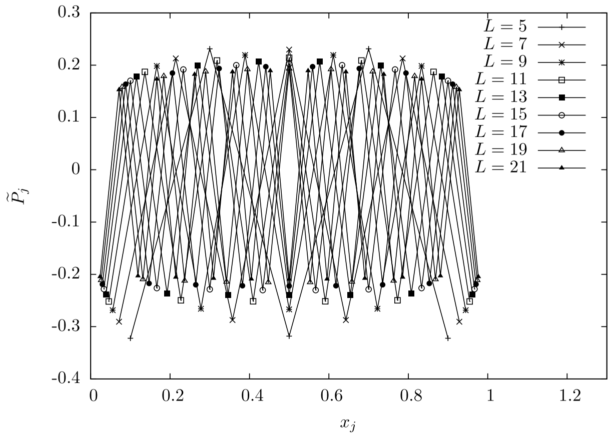

Fig. 6 Oscillatory part of the left-passage probability

Schramm's formula. Finite-size effects are more important near the boundaries, but as we already noted in Sect. 4, the scaling of $P_{1/2}$ with L is as predicted by Schramm's formula.

Finally, in Fig. 6, we plot the oscillatory part $\widetilde{P}_j$. This quantity is a lattice effect, and is not predicted directly by Schramm's formula.

5.3 Left-Passage Probability in the FK Model

5.3.1 Mapping to the Six-Vertex Model

Throughout this section, we remove the restriction on q, and we use the algebraic Bethe ansatz notation

$$q = \mathrm{e}^{\eta}, \qquad z_j = \mathrm{e}^{-v_j}, \qquad w = \mathrm{e}^{-u}.$$

Moreover, we introduce for convenience $\eta' := \eta + i\pi$, so that the loop weight reads

$$n = -\left(q + q^{-1}\right) = -2\cosh\eta = 2\cosh\eta'.$$

Following [2], we distribute the loop weight locally by orienting the loops: to each $\pi/2$ left (resp. right) turn of a loop, we associate a phase factor $\mathrm{e}^{\eta'/4}$ (resp. $\mathrm{e}^{-\eta'/4}$) in the

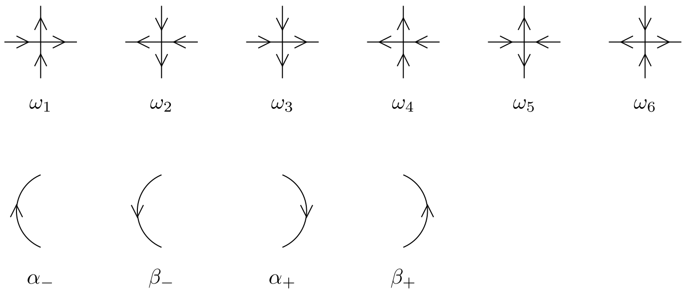

Fig. 7 The configurations of the six-vertex model and the associated Boltzmann weights

Boltzmann weights. Ignoring the loop connectivities results in a six-vertex (6V) model (see Fig. 7). Using the Boltzmann weights defined by the R-matrix in Definition 3.1 (with $z=1$ w.l.o.g. for the moment), the 6V weights can be rescaled to

$$\begin{aligned}
\omega_1 = \omega_2 &= \sinh(\eta+u), \\
\omega_3 = \omega_4 &= \sinh u, \\
\omega_5 &= \mathrm{e}^{+\eta'/2+u}\sinh\eta, \\
\omega_6 &= \mathrm{e}^{-\eta'/2-u}\sinh\eta.
\end{aligned} \tag{5.1}$$

Moreover, on the boundary, the loops undergo a half-turn, and hence the boundary weights must be

$$\alpha_\pm = \mathrm{e}^{-\eta'/2}, \qquad \beta_\pm = \mathrm{e}^{+\eta'/2}. \tag{5.2}$$

Hence the 6V model resulting from this mapping is described by the matrices

$$\underline{R}(u) = \begin{pmatrix} \sinh(\eta+u) & 0 & 0 & 0 \\ 0 & \sinh u & \mathrm{e}^{-\frac{\eta'}{2}-u}\sinh\eta & 0 \\ 0 & \mathrm{e}^{\frac{\eta'}{2}+u}\sinh\eta & \sinh u & 0 \\ 0 & 0 & 0 & \sinh(\eta+u) \end{pmatrix},$$

$$\underline{K}_\pm = \begin{pmatrix} \mathrm{e}^{-\frac{\eta'}{2}} & 0 \\ 0 & \mathrm{e}^{\frac{\eta'}{2}} \end{pmatrix},$$

and the corresponding transfer matrix is denoted by $\underline{t}_{6\mathrm{V}}$. These matrices are related to the standard 6V ones by the "gauge transformation"

$$\begin{aligned}
\underline{R}_{ab}(u-v) &= \mathrm{e}^{-(\frac{u}{2}+\frac{\eta'}{4})\sigma_a^z - \frac{v}{2}\sigma_b^z} R_{ab}(u-v)\mathrm{e}^{(\frac{u}{2}+\frac{\eta'}{4})\sigma_a^z + \frac{v}{2}\sigma_b^z} \\
&= \mathrm{e}^{-\frac{u}{2}\sigma_a^z - (\frac{v}{2}-\frac{\eta'}{4})\sigma_b^z} R_{ab}(u-v)\mathrm{e}^{\frac{u}{2}\sigma_a^z + (\frac{v}{2}-\frac{\eta'}{4})\sigma_b^z}, \\
\underline{K}_\pm &= \mathrm{e}^{\pm(u/2+\eta'/4)\sigma^z} K_\pm(u)\mathrm{e}^{\pm(u/2+\eta'/4)\sigma^z},
\end{aligned} \tag{5.3}$$

where a and b denote the two vector spaces acted on by R, $K_+(u) = 2e^{\xi_+} K(u+\eta, \xi_+)$, $K_-(u) = 2e^{\xi_-} K(u, \xi_-)$, and

$$R(u) = \begin{pmatrix} \sinh(\eta+u) & 0 & 0 & 0 \\ 0 & \sinh u & \sinh\eta & 0 \\ 0 & \sinh\eta & \sinh u & 0 \\ 0 & 0 & 0 & \sinh(\eta+u) \end{pmatrix},$$

$$K(u,\xi) = \begin{pmatrix} \sinh(\xi+u) & 0 \\ 0 & \sinh(\xi-u) \end{pmatrix},$$

with the values of the boundary parameters: $\xi_\pm = \mp\infty$. It is customary to shift the spectral parameters to define the monodromy matrices [26]:

$$u := \lambda - \eta/2, \qquad v_j := \xi_j - \eta/2,$$

and we thus write:

$$\begin{aligned} T(\lambda) &:= R_{0L}(\lambda-\xi_L)\dots R_{01}(\lambda-\xi_1), \\ \widehat{T}(\lambda) &:= R_{10}(\lambda+\xi_1-\eta)\dots R_{L0}(\lambda+\xi_L-\eta), \\ t_{6\mathrm{V}}(\lambda) &:= \mathrm{Tr}_0\big[K_+(\lambda)T(\lambda)K_-(\lambda)\widehat{T}(\lambda)\big]. \end{aligned} \tag{5.4}$$

One can easily show that the transfer matrices before and after the gauge change (5.3) are simply related by a similarity transformation

$$\underline{t}_{6\mathrm{V}} = G^{-1} t_{6\mathrm{V}} G, \quad \text{where } G := \prod_{j=1}^{L} e^{v_j \sigma_j^z/2}. \tag{5.5}$$

If we specialise to a homogeneous system where all the ξ_j's are set to $\eta/2$, the highly anisotropic limit $\lambda \to \eta/2$ yields the open XXZ Hamiltonian

$$\begin{aligned} \mathcal{H}_{\mathrm{XXZ}} &:= \left.\frac{\partial \log t_{6\mathrm{V}}(\lambda)}{\partial\lambda}\right|_{\lambda=\eta/2} \\ &= \sum_{j=1}^{L-1}\big[\sigma_j^x\sigma_{j+1}^x + \sigma_j^y\sigma_{j+1}^y + \cosh\eta\,\sigma_j^z\sigma_{j+1}^z\big] - \sinh\eta\big(\sigma_1^z - \sigma_L^z\big). \end{aligned} \tag{5.6}$$

Note that in the critical regime ($\eta \in i\mathbb{R}$), the boundary terms are imaginary. In the remainder of this section, we shall restrict ourselves to the homogeneous system described by $\mathcal{H}_{\mathrm{XXZ}}$, but our results can be readily generalised to an arbitrary choice of the ξ_j's.

5.3.2 The Left-Passage Probability as an XXZ Correlation Function

Proposition 5.5 *In the critical regime $\eta \in i\mathbb{R}$, the following identity holds*:

$$P_{j+1/2} = \sum_{\ell=1}^{j} \mathrm{Re}\left(\frac{\langle\Psi_0|\sigma_\ell^z|\Psi_0\rangle}{\langle\Psi_0|\Psi_0\rangle}\right), \tag{5.7}$$

where $\langle\Psi_0|$ and $|\Psi_0\rangle$ are the left and right eigenvectors of $\mathcal{H}_{\mathrm{XXZ}}$ (5.6) associated to the lowest energy.

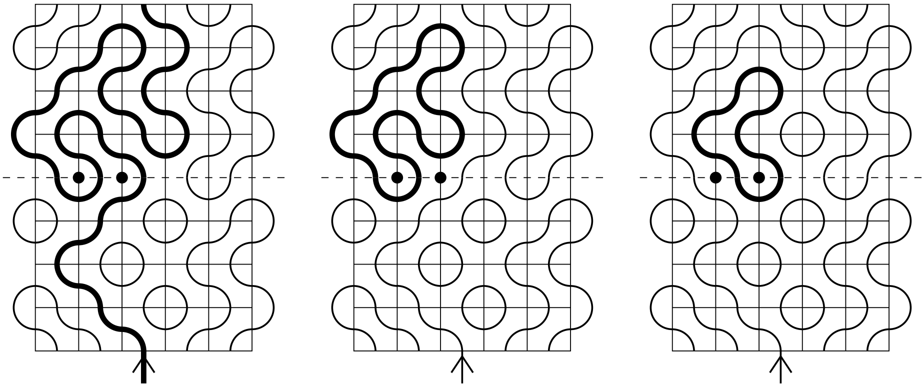

Fig. 8 From *left* to *right*: loop configurations belonging to the subsets $\mathcal{A}_j$, $\mathcal{A}'_j$, and $\mathcal{A}''_j$, for $j=2$ and $L=5$

Proof We have used the mapping of TL loop configurations to 6V arrow configurations described above, through the orientation of loops. Consider the intermediate model, i.e., the oriented TL (OTL) loops. In this model, a configuration C on the whole lattice has a Boltzmann weight (at the isotropic point $\lambda = -i\pi/2$)

$$W[C] = (-q)^{\#\text{anti-clockwise loops(C)}} \times (-1/q)^{\#\text{clockwise loops(C)}},$$

and the partition function is equal to that of the original TL model

$$\mathcal{Z}_{\text{OTL}} = \sum_{\text{oriented config. } C} W[C] = \sum_{\text{unoriented config. C}} \left(-q-q^{-1}\right)^{\#\text{loops}(C)} = \mathcal{Z}_{\text{TL}}.$$

We now consider a horizontal section of the strip, of the type shown in Fig. 2a. For a given oriented loop configuration C, we denote by $\sigma_j^z(C) \in \{1,-1\}$ the orientation of the arrow across the j-th horizontal edge. There are three possibilities for the loop passing through this edge (see Fig. 8):

- The loop is the open path γ. Then $\sigma_j^z(C) = (-1)^{j-1}$.
- The loop encloses the marked point on the left of j. Then $\sigma_j^z(C) = +1$ iff the loop is oriented anti-clockwise.
- The loop encloses the marked point on the right of j. Then $\sigma_j^z(C) = +1$ iff the loop is oriented clockwise.

We denote by $\mathcal{A}_j, \mathcal{A}'_j, \mathcal{A}''_j$ the corresponding subsets of oriented loop configurations. The expectation value of σ_j^z in the OTL model then reads

$$\begin{aligned}\langle\sigma_j^z\rangle_{\text{OTL}} &= \frac{1}{\mathcal{Z}}\left[(-1)^{j-1}\sum_{C\in\mathcal{A}_j} + \tanh\eta\left(\sum_{C\in\mathcal{A}'_j} - \sum_{C\in\mathcal{A}''_j}\right)\right]W[C] \\ &= (-1)^{j-1}X_j + \tanh\eta\left(\mathbb{P}\left[C\in\mathcal{A}'_j\right] - \mathbb{P}\left[C\in\mathcal{A}''_j\right]\right). \qquad (5.8)\end{aligned}$$

Finally, from the mapping between the TL loop model and the 6V model described above, we have

$$\frac{\langle\Psi_0|\sigma_j^z|\Psi_0\rangle}{\langle\Psi_0|\Psi_0\rangle} = \langle\sigma_j^z\rangle_{\text{OTL}}. \qquad \square$$

6 Discussion

In the percolation model, we have obtained an exact expression for the boundary passage probabilities P_b and $\widehat{P}_b$, which are lattice analogs of a boundary observable in SLE_6. In the FK cluster model with generic Q, we have related the left-passage probability to the magnetisation in a solvable open XXZ spin chain.

Our results have many possible developments. First, within the qKZ approach, we hope to exploit the symmetry and recursion relations for the probabilities X_j, $\widehat{X}_j$ and Y_j to find their explicit expressions. This certainly involves a deeper understanding of the properties of symplectic characters and Schur functions [14]. Second, with the algebraic Bethe ansatz [18, 19], it seems possible to calculate the magnetisation $\langle \sigma_j^z \rangle$ in the open XXZ chain in a closed form, at least for j close enough to one of the boundaries. The advantage of this method is that it is valid for any value of the deformation parameter q, and, in cases where a closed form cannot be achieved, it still produces determinant forms that can be evaluated numerically for very large system sizes ($L \sim 1000$ sites). Finally, we note that the probabilities X_j, $\widehat{X}_j$ and Y_j are very similar to the discretely holomorphic parafermions found for the TL loop model [17, 23], which are the starting point in the proof of conformal invariance for the Ising model [6, 28]. Thus the study of these objects on a general domain Ω may allow progress in extending this proof to the FK model with generic Q.

Acknowledgements The authors thank J. de Gier, C. Hagendorf, A. Mays, V. Terras, and P. Zinn-Justin for fruitful discussions. This work was supported by the European Research Council (grant CONFRA 228046).

References

1. Bauer, M., Bernard, D.: SLE martingales and the Virasoro algebra. Phys. Lett. B **557**(3–4), 309–316 (2003). doi:10.1016/S0370-2693(03)00189-8
2. Baxter, R.J.: Exactly Solved Models in Statistical Mechanics, 2nd edn. Dover, New York (2007). Reprint of the 1982 original, Academic Press, London
3. Cantini, L., Sportiello, A.: Proof of the Razumov–Stroganov conjecture. J. Comb. Theory, Ser. A **118**(5), 1549–1574 (2011). doi:10.1016/j.jcta.2011.01.007. arXiv:1003.3376v1
4. Cardy, J.: Critical percolation in finite geometries. J. Phys. A **25**(4), L201 (1992)
5. Cardy, J.: Network models in class C on arbitrary graphs. Commun. Math. Phys. **258**, 87–102 (2005). doi:10.1007/s00220-005-1304-y
6. Chelkak, D., Smirnov, S.: Universality in the 2D Ising model and conformal invariance of fermionic observables. Invent. Math. **189**(3), 515–580 (2012). arXiv:0910.2045
7. Di Francesco, P.: Inhomogeneous loop models with open boundaries. J. Phys. A **38**(27), 6091–6120 (2005)
8. Di Francesco, P.: Open boundary quantum Knizhnik–Zamolodchikov equation and the weighted enumeration of plane partitions with symmetries. J. Stat. Mech. **2007**, P01024 (2007). doi:10.1088/1742-5468/2007/01/P01024. arXiv:math-ph/0611012v2
9. Di Francesco, P., Saleur, H., Zuber, J.B.: Relations between the Coulomb gas picture and conformal invariance of two-dimensional critical models. J. Stat. Phys. **49**, 57–79 (1987). doi:10.1007/BF01009954
10. Di Francesco, P., Zinn-Justin, P.: Around the Razumov–Stroganov conjecture: proof of a multi-parameter sum rule. Electron. J. Comb. **12** (2005)
11. Di Francesco, P., Zinn-Justin, P.: Quantum Knizhnik–Zamolodchikov equation: reflecting boundary conditions and combinatorics. J. Stat. Mech. **2007**, P12009 (2007). doi:10.1088/1742-5468/2007/12/P12009
12. de Gier, J.: Loops, matchings and alternating-sign matrices. Discrete Math. **298**(1–3), 365–388 (2005). arXiv:math.CO/0211285v2
13. de Gier, J., Nienhuis, B., Ponsaing, A.K.: Exact spin quantum Hall current between boundaries of a lattice strip. Nucl. Phys. B **838**(3), 371–390 (2010). doi:10.1016/j.nuclphysb.2010.05.019. arXiv:1004.4037
14. de Gier, J., Ponsaing, A.K.: Separation of variables for symplectic characters. Lett. Math. Phys. **97**, 61–83 (2011). doi:10.1007/s11005-011-0467-z. arXiv:1009.2831v1

15. de Gier, J., Ponsaing, A.K., Shigechi, K.: The exact finite size ground state of the O $(n=1)$ loop model with open boundaries. J. Stat. Mech. **2009**(04), P04010 (2009). arXiv:0901.2961
16. de Gier, J., Pyatov, P.: Factorised solutions of Temperley–Lieb qKZ equations on a segment. Adv. Theor. Math. Phys. **14**, 795–877 (2010). arXiv:0710.5362 [math-ph]
17. Ikhlef, Y., Cardy, J.: Discretely holomorphic parafermions and integrable loop models. J. Phys. A **42**, 10 (2009)
18. Kitanine, N., Kozlowski, K.K., Maillet, J.M., Niccoli, G., Slavnov, N.A., Terras, V.: Correlation functions of the open XXZ chain: I. J. Stat. Mech. **2007**(10), P10009 (2007)
19. Kitanine, N., Kozlowski, K.K., Maillet, J.M., Niccoli, G., Slavnov, N.A., Terras, V.: Correlation functions of the open XXZ chain: II. J. Stat. Mech. **2008**(07), P07010 (2008)
20. Nienhuis, B.: Critical behavior of two-dimensional spin models and charge asymmetry in the Coulomb gas. J. Stat. Phys. **34**, 731–761 (1984). doi:10.1007/BF01009437
21. Razumov, A.V., Stroganov, Y.G.: Combinatorial nature of the ground-state vector of the O(1) loop model. Theor. Math. Phys. **138**(3), 333–337 (2004). doi:10.1023/B:TAMP.0000018450.36514.d7
22. Razumov, A.V., Stroganov, Y.G.: O(1) loop model with different boundary conditions and symmetry classes of alternating-sign matrices. Theor. Math. Phys. **142**(2), 237–243 (2005). doi:10.1007/s11232-005-0007-z
23. Riva, V., Cardy, J.: Holomorphic parafermions in the Potts model and stochastic Loewner evolution. J. Stat. Mech. **2006**(12), P12001 (2006)
24. Saleur, H., Duplantier, B.: Exact determination of the percolation hull exponent in two dimensions. Phys. Rev. Lett. **58**(22), 2325–2328 (1987). doi:10.1103/PhysRevLett.58.2325
25. Schramm, O.: A percolation formula. Electron. Commun. Probab. **6**, 115–120 (2001). arXiv:math/0107096
26. Sklyanin, E.K.: Boundary conditions for integrable quantum systems. J. Phys. A **21**(10), 2375–2389 (1988)
27. Smirnov, S.: Critical percolation in the plane: conformal invariance, Cardy's formula, scaling limits. C. R. Acad. Sci. Paris Ser. I Math. **333**(3), 239–244 (2001). doi:10.1016/S0764-4442(01)01991-7
28. Smirnov, S.: Conformal invariance in random cluster models I. Holomorphic fermions in the Ising model. Ann. Math. **172**(2), 1435–1467 (2010). doi:10.4007/annals.2010.172.1435. arXiv:0708.0039v1
29. Werner, W.: Percolation et modèle d'Ising. Cours Spécialisés [Specialized Courses], vol. 16. Société Mathématique de France, Paris (2009)
30. Zinn-Justin, P.: Private Communication
31. Zinn-Justin, P.: Loop model with mixed boundary conditions, qKZ equation and alternating sign matrices. J. Stat. Mech. **2007**(1), P01007 (2007). doi:10.1088/1742-5468/2007/01/P01007. arXiv:math-ph/0610067